Cell Tissue Res (2011) 343:429–444
DOI 10.1007/s00441-010-1098-x

REGULAR ARTICLE

Expression of lymphatic endothelium-specific hyaluronan receptor LYVE-1 in the developing mouse kidney

Hyun-Wook Lee · Yan-Xia Qin · Yu-Mi Kim · Eun-Young Park · Jin-Sun Hwang · Guan-Hua Huo · Chul-Woo Yang · Wan-Young Kim · Jin Kim

Received: 7 July 2010 / Accepted: 25 November 2010 / Published online: 23 December 2010

Abstract Our knowledge of the embryonic development of the lymphatic vessels within the kidney is limited. The aim of this study was to establish the time of appearance and the distribution of intra-renal lymphatic vessels in the developing mouse kidney by using the lymphatic marker, LYVE-1. Kidneys from embryonic day 12 (E12) to E18, from neonates at post-natal day 1 (P1) to P21, and from adults were studied. In the adult mouse kidney, LYVE-1 was expressed mainly in the lymphatic endothelial cells (LECs) and in a subset of endothelial cells in the glomerular capillaries. However, in the developing mouse kidney, LYVE-1 was also expressed transiently in F4/80$^+$/CD11b$^-$ immature macrophages/dendritic cells and in the developing renal vein. LYVE-1$^+$ lymphatic vessels connected with extra-renal lymphatics were detected in the kidney at E13. F4/80$^+$/CD11b$^-$/LYVE-1$^+$ immature macrophages/dendritic cells appeared prior to the appearance of LYVE-1$^+$ renal lymphatic vessels and were closely intermingled or even formed part of the lymphatic vascular wall. Prox1 was expressed only in the LYVE-1$^+$ LECs from fetus to adulthood, but not in LYVE-1$^+$ endothelial cells of the developing renal vein and macrophages/dendritic cells. Thus, lymphatic vessels of the kidney might originate by extension of extra-renal lymphatics through an active branching process possibly associated with F4/80$^+$/CD11b$^-$/LYVE-1$^+$ macrophages/dendritic cells.

Keywords LYVE-1 · Lymphangiogenesis · Kidney · Mouse (C57BL/6)

Hyun-Wook Lee and Yan-Xia Qin contributed equally to this work. Some of this work has been published in abstract form (J Am Soc Nephrol 17:TH-PO644, 2006) and presented at the Renal Week 2006 Meeting, San Diego, Calif., USA, November 16–19, 2006.

This work was supported by the Korea Science and Engineering Foundation (R13-2002-005-03001-0) through the Medical Research Center for Cell Death Disease Research Center at The Catholic University of Korea.

The authors declare no conflicts of interest.

Electronic supplementary material The online version of this article (doi:10.1007/s00441-010-1098-x) contains supplementary material, which is available to authorized users.

H.-W. Lee · Y.-M. Kim · E.-Y. Park · J.-S. Hwang · W.-Y. Kim · J. Kim (✉)
Department of Anatomy and MRC for Cell Death Disease Research Center, College of Medicine,
The Catholic University of Korea,
505, Banpo-Dong, Seocho-Ku,
Seoul 137-701, Korea
e-mail: jinkim@catholic.ac.kr

C.-W. Yang
Department of Internal Medicine and Cell Death Disease Research Center, College of Medicine, The Catholic University of Korea, Seoul, Korea

Y.-X. Qin · G.-H. Huo
Department of Histology and Embryology,
Binzhou Medical University,
Binzhou, China

Introduction

The renal lymphatics contribute to the drainage of leaked plasma and interstitial fluid under normal and abnormal physiological conditions (Madsen et al. 2008; Rohn et al. 1996). The distribution of the normal renal lymphatic system has been investigated in various animals including the human and mouse (Cuttino et al. 1985; Hogg et al. 1982; Holmes et al. 1977). Intra-renal lymphatics are embedded in the periarterial loose connective tissue around the renal arteries and are distributed primarily along the interlobular and arcuate arteries in the cortex. However, the

renal medulla has no lymphatic drainage (Madsen et al. 2008). Our knowledge of the distribution of lymphatics within the developing kidney has been restricted because of the lack of a reliable marker that can distinguish the lymphatic endothelium from that of the blood capillaries.

Lymphatic vessels were first described at the beginning of the seventeenth century, but the first growth factors and molecular markers specific for these vessels were discovered only 10 years ago. More recently, certain proteins specific for lymphatic endothelial cells (LECs) have been identified, including lymphatic endothelial hyaluronan receptor-1 (LYVE-1), vascular endothelial growth factor receptor (VEGFR)-3, prospero-related homeobox gene-1 (Prox1), and podoplanin (Hirakawa and Detmar 2004; Oliver 2004; Oliver and Alitalo 2005; Tammela et al. 2005). However, the widespread localization of some of these markers has revealed that their specificity is not stringent. Thus, VEGFR-3 can also be expressed in blood vascular endothelium (Kubo et al. 2000; Niki et al. 2001). Podoplanin is a mucin-type transmembrane glycoprotein that is expressed not only in LECs, but also in renal podocytes, epithelial cells of the choroid plexus, keratinocytes, and alveolar type I cells in the lung and in other cells (Alitalo et al. 2005; Al-Rawi et al. 2005; Oliver and Alitalo 2005; Schacht et al. 2005). In contrast, LYVE-1 is now a commonly used marker for lymphatic endothelium and currently provides the first indicator of lymphatic endothelial competence (Jackson 2004; Jurisic and Detmar 2009; Maby-El Hajjami and Petrova 2008). LYVE-1 is a transmembrane glycoprotein that contains an extracellular matrix glycosaminoglycan hyaluronan-binding domain and binds to both immobilized and soluble hyaluronan (Banerji et al. 1999; Beasley et al. 2002; Prevo et al. 2001). LYVE-1 shares 41% homology with the leukocyte homing receptor CD44 molecule, which supports hyaluronan-mediated rolling on inflamed hemovascular endothelium (Pure and Cuff 2001). The highly selective expression of LYVE-1 in the lymphatics is probably attributable to the important role of the lymphatic system in the metabolism of hyaluronan. More than 80% of tissue hyaluronan is degraded within the lymph nodes. LYVE-1 is probably a key receptor responsible for the uptake and transport of hyaluronan in the lymph. LYVE-1 expression remains almost exclusively confined to lymphatic vessels and to the sinus endothelium of the lymph node (Oliver and Detmar 2002; Oliver 2004). These latter properties have made LYVE-1 a powerful and widely exploited molecular marker in studies of embryonic and pathological lymphangiogenesis.

Prox1 is known as a master regulator of lymphatic endothelial differentiation. In mice, Prox1 begins to be expressed almost simultaneously with LYVE-1 in the subpopulation of venous endothelial cells that, by budding and sprouting, give rise to the lymphatic system. These findings fully validate Sabin's proposal of the venous origin of the primary lymphatic sacs (Sabin 1909; Wigle and Oliver 1999; Wigle et al. 2002).

Interestingly, LYVE-1 is also expressed in a subset of macrophages (Grant et al. 2002; Mouta Carreira et al. 2001), and these LYVE-1^+ macrophages might play a role in lymphangiogenesis (Hamrah et al. 2004; Maruyama et al. 2005; Schledzewski et al. 2006).

To date, no report of LYVE-1 expression in the developing kidney has been presented. Therefore, the purpose of this study has been to identify and characterize LYVE-1 expression and to establish the distribution of intrarenal lymphatic vessels in the developing mouse kidney. In addition, we present the first study showing whether renal lymphatic vessels form by the dedifferentiation of LECs from venous endothelial cells and subsequent sprouting lymphangiogenesis, or whether they can also be formed by mesenchymal precursor cells, possibly macrophages, or by sprouting from pre-existing extra-renal lymphatic vessels.

Materials and methods

Animals and tissue preservation

C57BL/6 mice were used in all experiments. Animal care and experimental procedures were performed under approval from the Animal Care Committees of the Catholic University of Korea. Prenatal kidneys were obtained from 12-, 13-, 14-, 15-, 16-, and 18-day-old fetuses (embryonic day E12–E18), and postnatal kidneys were obtained from 1-, 4-, 7-, 14-, and 21-day-old pups (neonatal pup days P1–P21) and from adult (8-week-old male) animals. For each age group, three or four animals from two separate litters were used. The animals were anesthetized with an intraperitoneal injection of 16.5% urethane (1 ml/0.1 kg body weight). The kidneys of early prenatal animals were preserved by immersion fixation, and those of late prenatal or postnatal animals were fixed by in vivo perfusion through the heart. The kidneys were perfused briefly with phosphate-buffered saline (PBS; 298 mOsm/kg H_2O, pH 7.4) to rinse away all blood. This was followed by perfusion with periodate–lysine–2% paraformaldehyde (PLP) solution for 10 min. After perfusion, the kidneys were removed and cut into slices (1–2 mm thick), which were further fixed by immersion in the same fixative overnight at 4°C. Sections of tissue were cut transversely through the entire kidney at 50 μm by using a vibratome (Pelco 102, Series 1000; Technical Products International, St. Louis, Mo., USA). For the whole-mount staining of embryos and kidneys, tissues were fixed by immersion in the same fixative overnight at 4°C. They were processed for

immunohistochemical studies by using a horseradish-peroxidase pre-embedding technique.

Antibodies

Lymphatic vessels were detected by using affinity-purified rabbit polyclonal antibodies directed against LYVE-1 (1:1,000; Research Diagnostics, Flanders, N.J., USA) and Prox1 (1:1,000; Chemicon, Temecula, Calif., USA). The developing renal arteries were identified by using a rabbit polyclonal antibody against AQP1 (1:800; Chemicon; Kim et al. 1999). CD31 was employed to detect the endothelial cells of blood vessels (1:200; BD Bioscience, Franklin Lakes, N.J., USA), and alpha-smooth muscle actin (α-SMA; 1:1,000; Sigma-Aldrich, St. Louis, Mo., USA) to identify the smooth muscle actin surrounding arterial vessels. Macrophages were identified by means of a rat polyclonal antibody against F4/80 (1:30; Serotec, Oxford, UK). CD45 (1:50; BD Bioscience) was used to detect leukocytes. CD11b (1:50; BD Pharmingen, San Diego, Calif., USA) was employed because of its expression at variable levels on granulocytes, macrophages, and myeloid-derived dendritic cells. Nestin (1:2,000; Serotec) and vimentin (1:2,000; Dako, Glostrup, Denmark) were used as biomarkers of stem cells (Bouwens and DeBlay 1996; Lendahl et al 1990).

Immunohistochemistry: pre-embedding immunolabeling for LYVE-1

Sections of PLP-fixed tissue were cut transversely through the kidney on a vibratome at 50 μm and were processed for immunohistochemistry with an indirect immunoperoxidase method. All sections were washed three times in PBS containing 50 mM NH_4Cl for 15 min. Before incubation with the primary antibodies, the sections were pretreated with a graded series of ethanol (or not pretreated) and then incubated for 4 h with PBS containing 1% bovine serum albumin (BSA), 0.05% saponin, and 0.2% gelatin (solution A). The tissue sections were then incubated overnight at 4°C with antibodies directed against LYVE-1 (1:1,000) or AQP1 (1:800) diluted in solution A. After several washes in PBS containing 0.1% BSA, 0.05% saponin, and 0.2% gelatin (solution B), the tissue sections were incubated for 2 h in horseradish-peroxidase-conjugated donkey anti-rabbit IgG FaB fragment (Jackson ImmunoResearch Laboratories, West Grove, Pa., USA) diluted 1:100 in PBS containing 1% BSA. The tissues were then rinsed, first in solution B and then in 0.05 M TRIS buffer (pH 7.6). To detect horseradish peroxidase, the sections were incubated in 0.1% 3,3′-diaminobenzidine (DAB) in 0.05 M TRIS buffer for 5 min. Then, H_2O_2 was added to give a final concentration of 0.01%, and the incubation was continued for 10 min. The sections were washed three times with 0.05 M TRIS buffer, dehydrated in a graded series of ethanol, and mounted in Poly/Bed 812 resin (Polysciences, Warrington, Calif., USA). The sections were examined with a light microscope. For electron microscopy, the vibratome sections were postfixed with 1% glutaraldehyde and 1% osmium tetroxide in 0.1 M phosphate buffer, before being dehydrated and mounted in Poly/Bed 812 resin between polyethylene vinyl sheets. Ultrathin sections were stained with uranyl acetate and photographed by using a JEOL JEM-1010 transmission electron microscope (JEOL, Tokyo, Japan).

Immunohistochemistry: whole-mount immunolabling for LYVE-1

Some embryo (E12) and kidney (E13) were processed for whole-mount staining for LYVE-1. Before incubation with the primary antibodies, the embryos or kidneys were incubated overnight with PBS containing 1% BSA, 1% Triton X-100, and 0.2% gelatin (solution C). The embryos or kidneys were then incubated for 2 days at 4°C with antibodies directed against LYVE-1 (1:1,000) diluted in solution C. After several washes in PBS containing 0.1% BSA, 1% Triton X-100, and 0.2% gelatin (solution D), the embryos or kidneys were incubated overnight in horseradish-peroxidase-conjugated donkey anti-rabbit IgG FaB fragment (Jackson ImmunoResearch Laboratories) diluted 1:100 in PBS containing 1% BSA and 1% Triton X-100. The embryos or kidneys were then rinsed, first in solution D and then in 0.05 M TRIS buffer (pH 7.6). To detect horseradish peroxidase, the sections were incubated in 0.1% DAB in 0.05 M TRIS buffer for 5 min. Then, H_2O_2 was added to give a final concentration of 0.01%, and the incubation was continued for 10 min. The embryos or kidneys were washed three times with 0.05 M TRIS buffer and examined with a light microscope and Canon EOS 5D digital SLR camera (Canon, Tokyo, Japan).

Immunofluorescence for LYVE-1 and other antibodies

The procedure was the same as that in the pre-embedding methods before treatment with primary antibodies. For double- or triple-label immunofluorescence, anti-LYVE-1 was mixed with antibodies for Prox1 (1:1,000), F4/80 (1:30), CD45 (1:50), CD11b (1:50), nestin (1:2,000), vimentin (1:2,000), or CD31 (1:200). Labeling in mouse tissues was visualized by using Alexa488-conjugated donkey anti-rabbit antibody, Cy3-conjugated donkey anti-rat, or Cy3-conjugated donkey anti-mouse antibodies (all dilutions 1:1,000, Jackson ImmunoResearch Laboratories). Tissues were mounted in Vectashield mounting

medium (Vector Labs, Burlingame, Calif., USA) and viewed by immunofluorescence microscopy (Carl Zeiss, Jena, Germany) and Ziess LSM confocal microscopy (Carl Zeiss). Images were acquired by using a Zeiss LSM 510 confocal microscope (Carl Zeiss) and LSM 510 version 2.02 software. Optical sections with a Z-step size of 1 μm were generated and digitally merged to yield maximum projection images.

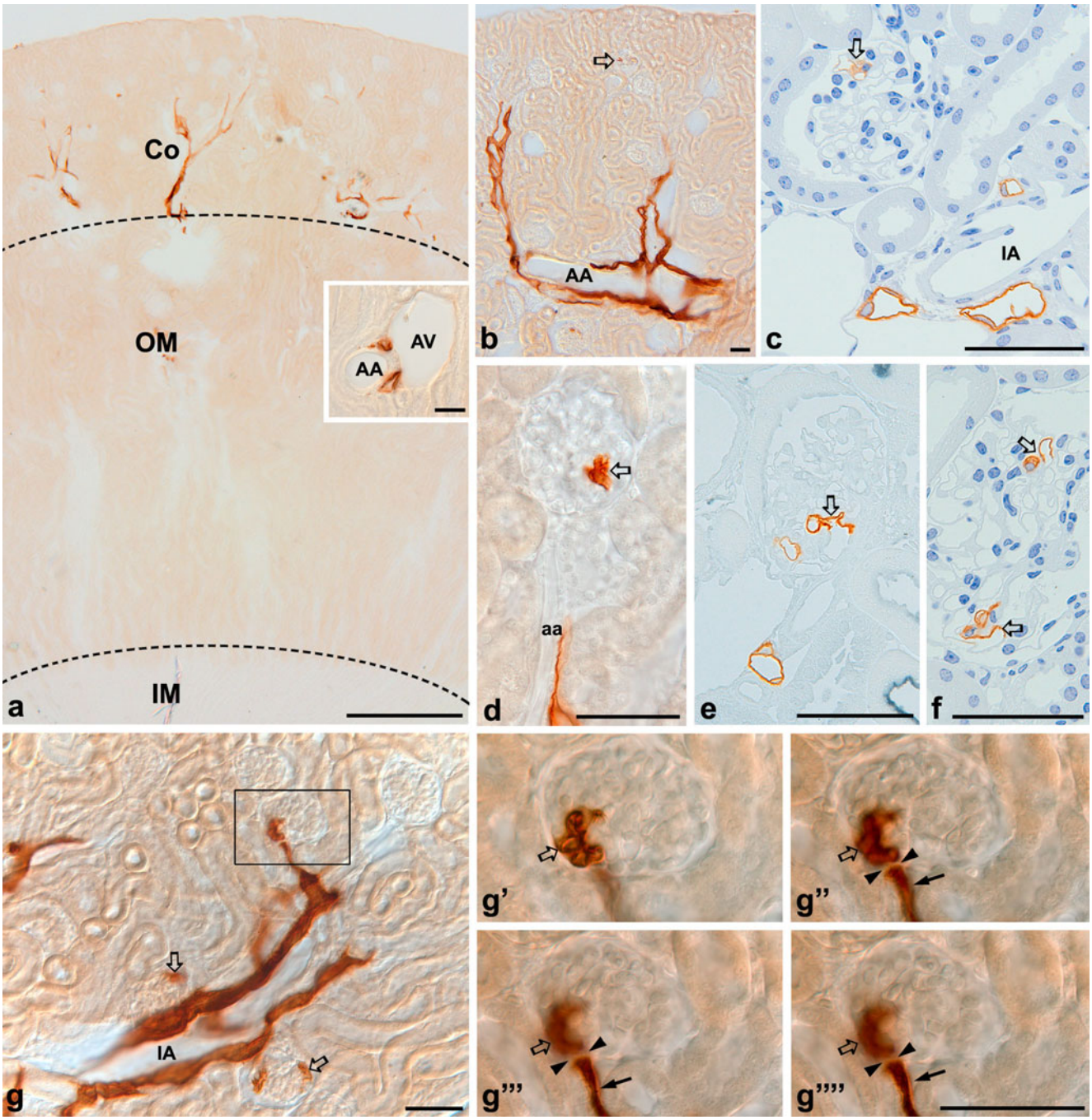

Fig. 1 Light micrographs of adult mouse kidney illustrating immunostaining for LYVE-1. The 50-μm vibratome sections and 1-μm plastic sections were stained for LYVE-1 by using pre-embedding (**a**, **b**, **d**, **g**–**g''''**) and post-embedding (**c**, **e**-**f**) methods. **a** Immunoreactivity for LYVE-1 was seen only in the cortex (*Co*), but not in the outer (*OM*) or inner (*IM*) medulla. *Inset* LYVE-1$^+$ lymphatic vessels around the arcuate artery (*AA*). Note the absence of immunoreactivity for LYVE-1 in the AA and arcuate vein (*AV*); the AA have thicker and more muscular walls than the AV. **b**–**d** LYVE-1$^+$ lymphatic vessels were distributed along the AA, interlobular artery (*IA*) and afferent arteriole (*aa*). **b**–**g** Note the LYVE-1$^+$ endothelial cells in the glomerulus (*open arrows*). **g'**–**g''''** Differently focused, higher magnification micrographs of the area indicated by the *boxed area* in **g** revealing the narrow gap (*arrowheads*) between LYVE-1$^+$ glomerular endothelial cells (*open arrow*) and an extraglomerular lymphatic capillary (*arrow*). *Bars* 1 mm (**a**), 50 μm(**b**–**g''''**)

Immunohistochemistry: post-embedding double-immunolabeling for LYVE-1 and α-SMA or AQP1

Vibratome sections were labeled with anti-LYVE-1 (1:1,000), with DAB as the chromogen (brown), as described above. Sections of each part of the kidney from flat-embedded 50-μm vibratome sections were glued onto empty blocks of Poly/Bed 812 resin. Anti-LYVE-1-labeled samples were cut into three consecutive sections and treated for 13 min with a mixture of saturated sodium hydroxide and absolute ethanol (1:1) to remove the resin. After three brief rinses in absolute ethanol, the sections were hydrated with graded ethanol and rinsed in tap water. They were then incubated for 30 min with methanolic H_2O_2, rinsed in tap water, and treated with 0.5% Triton X-100 in PBS for 15 min. The sections were then rinsed in PBS three times for 10 min before being treated with 1% BSA for 1 h. Two of the consecutive sections were incubated with α-SMA (1:2,000) and AQP1

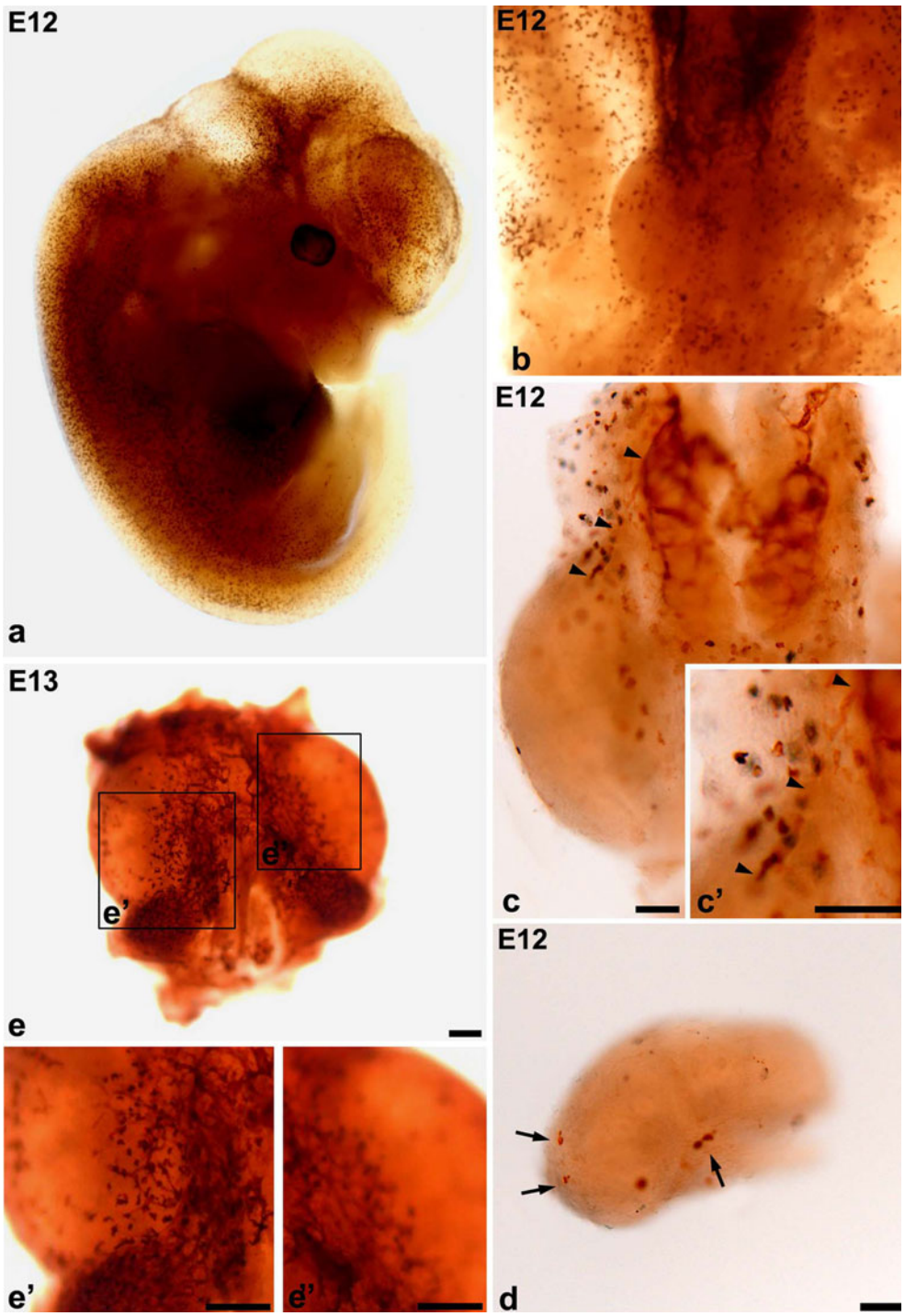

Fig. 2 Immunolocalization of LYVE-1 in developing mouse embryo (**a**) and kidneys (**b-e**) from 12-day-old (**a–d**) and 13-day-old (**e**, **e'**) fetuses. The embryos and kidneys were stained with LYVE-1 by whole-mount immunohistochemistry. **a** In 12-day-old embryo (*E12*), a large number of LYVE-1$^+$ single cells were distributed throughout the embryonic body. **b–d** Note the well-developed extra-renal lymphatic vessels with strong immunoreactivity for LYVE-1. No LYVE-1$^+$ lymphatic vessels were observed in the kidney at this age. Only a few LYVE-1$^+$ single cells (*arrows*) were observed (*arrowheads* weak LYVE-1 immunolabeling of a lymphatic vessel extending to kidney). **e** By E13, LYVE-1$^+$ extra-renal lymphatics had extended into the renal hilum. Note that many LYVE-1$^+$ single cells were closely intermingled around the lymphtic plexus. **e'**, **e"** Higher magnification views of the *boxed area* in **e**. *Bars* 100 μm

(1:1,000), respectively, whereas the third section was incubated in PBS overnight at 4°C. After being washed in PBS, the tissue sections were incubated for 2 h in horseradish-peroxidase-conjugated donkey anti-mouse IgG Fab fragment or donkey anti-rabbit IgG Fab fragment (Jackson ImmunoResearch Laboratories) diluted 1:200 in PBS. For the detection of peroxidase, Vector SG was used as the chromogen to produce a blue color easily distinguishable from the brown staining produced by DAB in the pre-embedding procedure for the detection of LYVE-1. One of the consecutive sections was counterstained with hematoxylin. The sections were washed with distilled water, dehydrated with graded ethanol and xylene, mounted in Canada balsam, and examined with a light microscope.

Quantification of LYVE-1$^+$ single cells in the interstitium

Cell counting was performed in kidney sections from the developing mouse by using digital images. Five fields from the cortex and five fields from the medulla were randomly

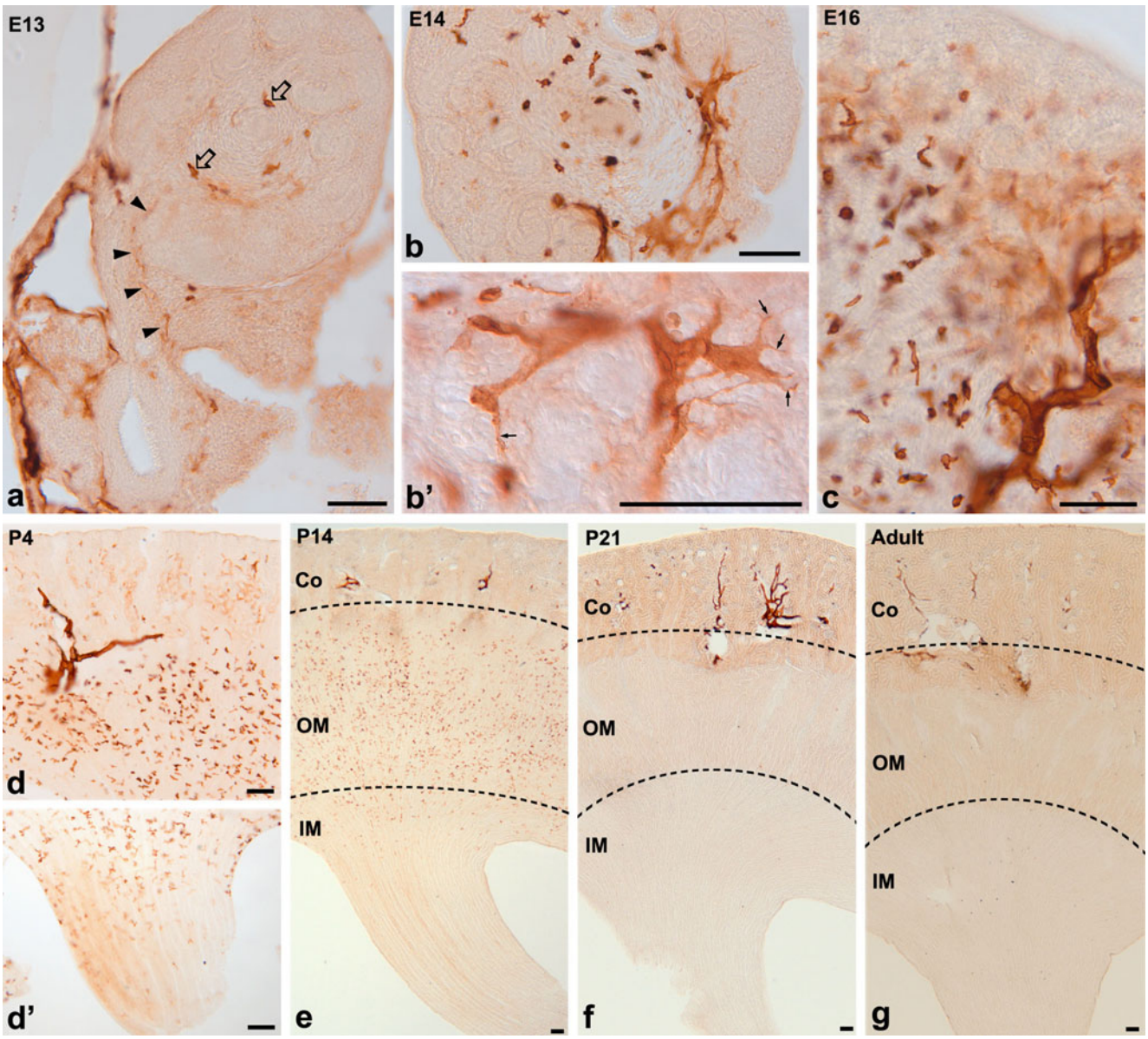

Fig. 3 Light micrographs of 50-μm vibratome sections illustrating immunostaining for LYVE-1 in mouse kidneys from 13-day-old (**a**), 14-day-old (**b**), and 16-day-old (**c**) fetuses, 4-day-old (**d**), 14-day-old (**e**), and 21-day-old (**f**) pups, and an adult (**g**). **a** Note the weak LYVE-1$^+$ lymphatic vessel (*arrowheads*) extending from extra-renal lymphatics, and the LYVE-1$^+$ single cells (*open arrows*) in the medulla. **b**, **b'** Well-developed LYVE-1$^+$ lymphatic plexuses were detected at E14 (*arrows* sprouts of growing lymphatic vessels in **b'**). **c**–**g** LYVE-1$^+$ lymphatic vessels formed gradually along the arcuate and interlobular blood vessels in the cortex (*Co*) during development (*OM* outer medulla, *IM* inner medulla). LYVE-1$^+$ single cells increased in number especially in the medulla until P4 (**c**, **d**), gradually decreased, and then completely disappeared at P21 (**f**), as in the adult kidney (**g**). **d'** LYVE-1$^+$ single cells in the renal papilla at P4. *Bars* 100 μm

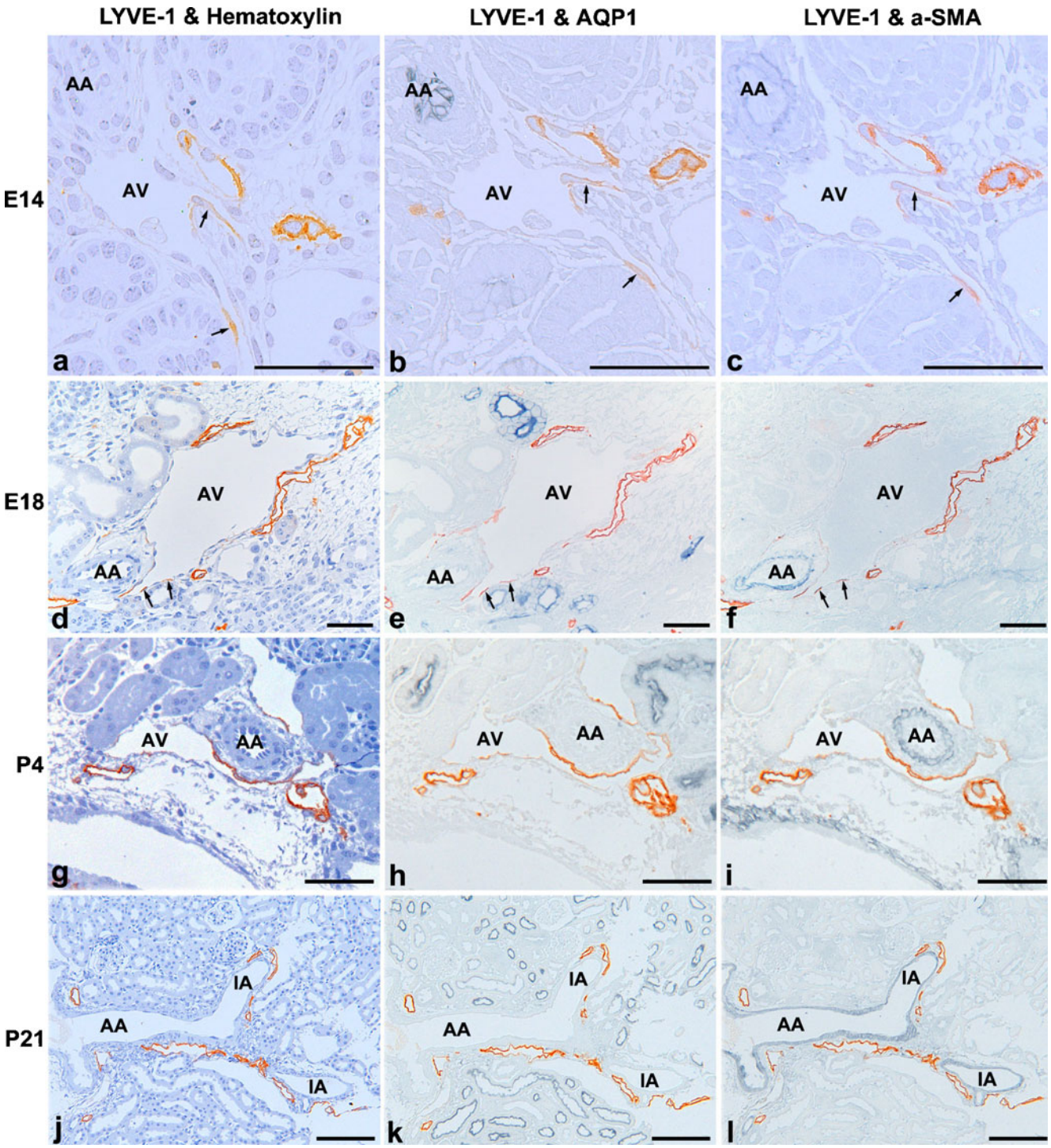

Fig. 4 Light micrographs of consecutive 1-μm plastic sections illustrating single immunostaining for LYVE-1 (*brown*; **a**, **d**, **g**, **j**) and double-immunostaining for LYVE-1 (*brown*) and AQP1 (*blue*; **b**, **e**, **h**, **k**) or LYVE-1 (*brown*) and α-SMA (*blue*; **c**, **f**, **i**, **l**) in mouse kidneys from 14-day-old (**a–c**) and 18-day-old (**d–f**) fetuses and 4-day-old (**g–i**) and 21-day-old (**j–l**) pups. **a–i** LYVE-1$^+$ lymphatic vessels appear around arcuate veins (*AV*). Note LYVE-1$^+$ endothelial cells (*arrows*) in branching buds *AV* but not in *AA* (arcuate arteries). α-SMA is extensively expressed in smooth muscle cells surrounding the arteries (**c**, **f**, **i**, **l**). **j–l** At P21, LYVE-1$^+$ lymphatic vessels are located around the AA and interlobular arteries (*IA*) with thick α-SMA$^+$ smooth muscles. AQP1 is expressed in the endothelial cells of the AA at E14 (**b**) and E18 (**d**) but disappears at P4 (**h**) and P21 (**k**). *Bars* 50 μm

selected from each of three animals in each age group. The total number of LYVE-1$^+$ single cells located in the interstitium in each field was counted and expressed per unit area of the field. Data are presented as means±SD.

Results

Immunohistochemical detection of LYVE-1 in adult mouse kidneys

LYVE-1 was expressed in the LECs and some endothelial cells of glomerular capillaries in the adult mouse kidney. LYVE-1$^+$ lymphatic vessels were located along the arterial system including the arcuate and interlobular arteries and the afferent arterioles (Fig. 1a-c). Interestingly, a few LYVE-1$^+$ endothelial cells were observed in the glomerular capillaries (Fig. 1d-g). The cells were confirmed as being vascular endotheial cells by the observation of red blood cells within the lumen of the glomerulus capillary that were composed of LYVE-1$^+$ endothelial cells (see Supplemental Figure S1). The localization and numbers of these LYVE-1$^+$ endothelial cells were variable in the glomerulus (Fig. 1g). The ends of the LYVE-1$^+$ lymphatic capillaries extended to Bowman's capsule of the renal corpuscle, but we never observed connections between LYVE-1$^+$ endo-

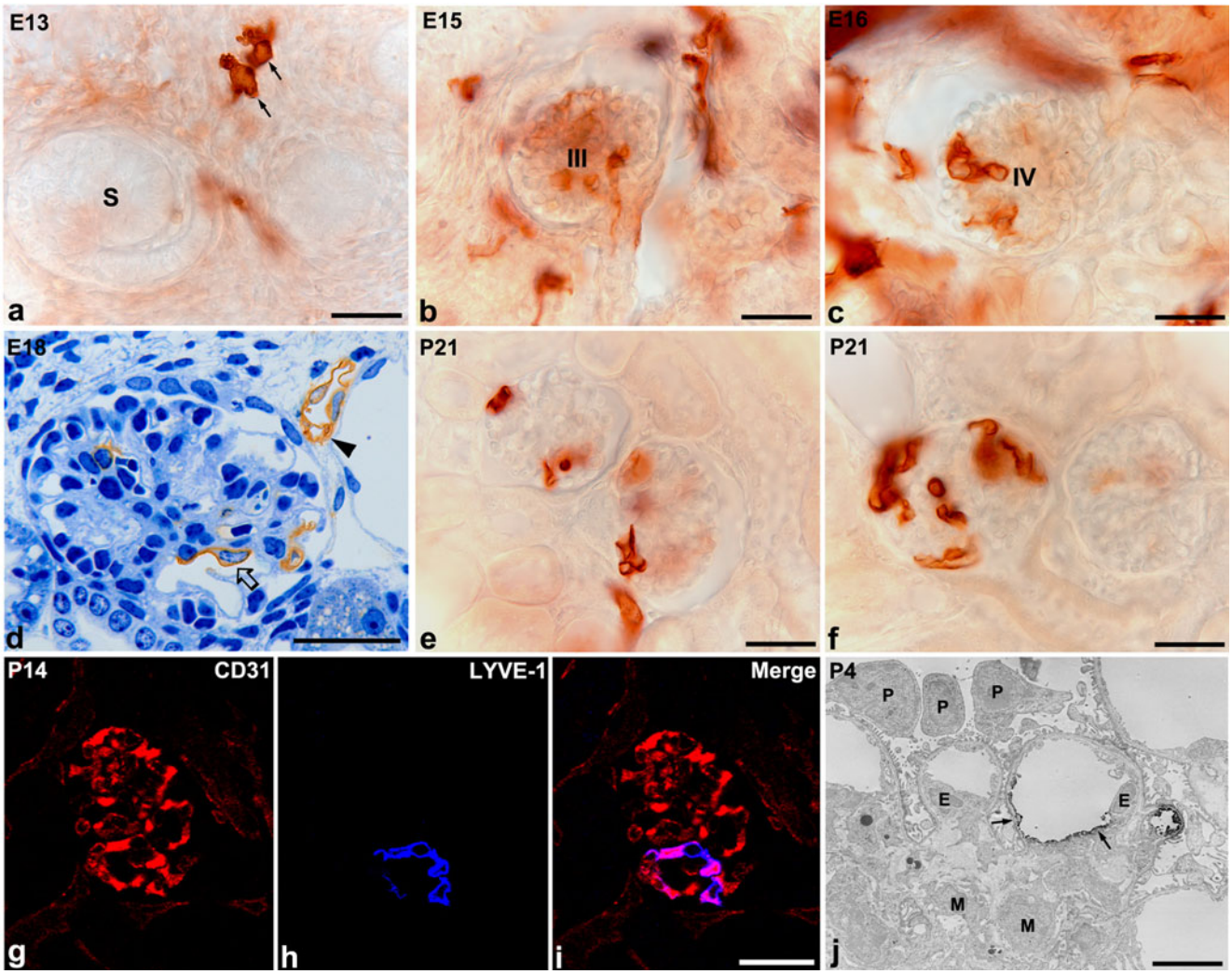

Fig. 5 Appearance of LYVE-1$^+$ endothelial cells in the developing glomerulus. **a** At E13, no immunoreactivity for LYVE-1 was observed in the early stage of the developing nephron including the S-shaped body (*S*). LYVE-1$^+$ single cells were present (*arrows*). **b**, **c** LYVE-1$^+$ endothelial cells appeared first in the glomerulus of stage III nephrons at E15 (**b**) and stage IV nephrons at E16 (**c**). **d** Plastic 1-μm section of the kidney from E18 showing LYVE-1$^+$ endothelial cells in the glomerulus (*open arrow*). Note a LYVE-1$^+$ lymphatic capillary (*arrowhead*) located adjacent to the Bowman's capsule. **e**, **f** Four glomeruli with variable numbers of LYVE-1$^+$ endothelial cells in the P21 kidney. **g–i** Double-immunofluorescence staining for LYVE-1 (*blue*) and CD31 (*red*) demonstrates overlapping reactivity in a subset of glomerular endothelial cells. **j** A few LYVE-1$^+$ endothelial cells (*arrows*) were observed in the glomerulus (*E* endothelial cell, *P* podocyte, *M* mesangial cell). *Bars* 30 μm (**a-i**), 5 μm (**j**)

thelial cells and lymphatic capillaries (Fig. 1g'-g''''). No LYVE-1$^+$ lymphatic vessels were observed in the medulla, and LYVE-1 was not expressed in the renal tubules or in the interstitium (Fig. 1a).

Immunohistochemical detection of LYVE-1 in developing mouse kidneys

In addition to the expression of LYVE-1 in the lymphatics and the glomerulus, LYVE-1$^+$ cells appeared transiently in cells in the interstitium and in the differentiating renal veins of the developing kidney.

LYVE-1 immunoreactivity in lymphatic vessels and in cells in the interstitium

In 12-day-old embryo, LYVE-1$^+$ single cells were distributed throughout the embryonic body (Fig. 2a). Although well-developed extra-renal LYVE-1$^+$ lymphatic plexuses were observed in E12, no LYVE-1$^+$ lymphatic vessels were observed within the kidney (Fig. 2b-d).

In the kidney of E13 animals, LYVE-1$^+$ extra-renal lymphatics had extended into the kidney and formed a rich plexus in the renal hilum (Fig. 2e-e''). At the corticomedullary junction at this age, weakly stained LYVE-1$^+$ lymphatic vessels were observed that were connected to strongly staining LYVE-1$^+$ extra-renal lymphatics (Fig. 3a). By E14, immunoreactivity for LYVE-1 had increased markedly in lymphatic vessels that formed a well-organized plexus and networks (Fig. 3b). Many filopodia-like sprouts occurred on the end of growing LYVE-1$^+$ lymphatic vessels (Fig. 3b'). LYVE-1$^+$ lymphatic vessel networks developed gradually along the growing arcuate and interlobular vessels (Fig. 3c-g). However, no LYVE-1$^+$ lymphatic vessels were observed in the renal medulla at any developmental stage (Fig. 3).

In addition to the expression of LYVE-1$^+$ in lymphatic vessels, strong immunoreactivity for LYVE-1 was observed in a few scattered individual cells, which were located mainly in the medulla. They were first observed at E12 (Fig. 2d) and gradually increased in number until P4 (Fig. 3b-d). The LYVE-1$^+$ single cells then disappeared gradually from the tip of the renal papilla (Fig. 3e) and were not observed at P21 (Fig. 3f) or in the adult kidney (Fig. 3g).

Relationship between LYVE-1$^+$ lymphatic vessels and differentiating renal veins in early developmental stages

To confirm the exact localization of LYVE-1$^+$ lymphatic vessels, three consecutive 1-μm-thick plastic sections immunostained for LYVE-1 by the pre-embedding method were immunostained for AQP1 or α-SMA. We have

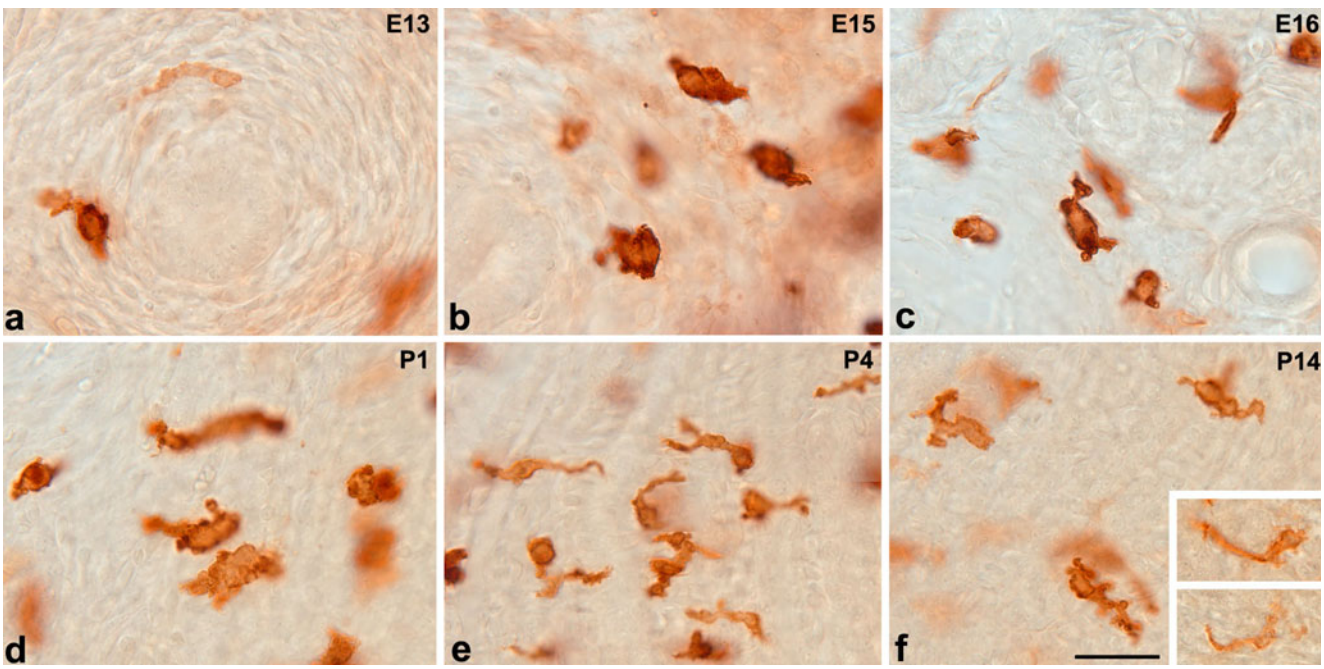

Fig. 6 High magnification micrographs from 13-day-old (**a**), 15-day-old (**b**), and 16-day-old (**c**) fetuses and 1-day-old (**d**), 4-day-old (**e**), and 14-day-old (**f**) pups showing morphological changes of LYVE-1$^+$ single cells at the light-microscope level. These cells had several thick, irregularly shaped, cytoplasmic processes, which decreased gradually in thickness but increased in length after birth. *Insets* in **f** LYVE-1$^+$ single cells with markedly decreased immunoreactivity located in the deeper portion of the inner medulla at P14. *Bars* 30 μm

previously demonstrated that AQP1 is expressed in arterial endothelial cells in early stages of development in the rat kidney (Kim et al. 1999). In the mouse, AQP1 was also expressed in the endothelial cells of developing arteries until P1 (Fig. 4b, e) and immunoreactivity for AQP1 in the arterial endothelial cells disappeared after P4 (Fig. 4h, k). However, AQP1 was not expressed in the developing venous endothelial cells (Fig. 4b, e, h, k).

LYVE-1$^+$ lymphatic vessels were mainly located around the developing veins in fetal and neonatal kidneys until P4 (Fig. 4a-i). In these early developing stages, scattered LYVE-1$^+$ endothelial cells were observed in the developing arcuate veins, mainly in the branching buds (Fig. 4a-i). From P7, LYVE-1$^+$ lymphatic vessels were found around the developing arcuate and interlobular arteries (Fig. 4j-l). No LYVE-1$^+$ endothelial cells were observed in the arterial system of the kidneys at any stage.

LYVE-1 immunoreactivity in endothelial cells in developing glomerulus

No immunoreactivity for LYVE-1 was detected in the vesicles of S-shaped bodies (Fig. 5a). LYVE-1$^+$ endothelial cells appeared first in the glomeruli of stage III nephrons at E15 (Fig. 5b). From E16, LYVE-1$^+$ endothelial cells appeared in the mature glomerulus (Fig. 5c), but the numbers and locations differed between glomeruli (Fig. 5d-f). Expression of LYVE-1 in a subset of CD31$^+$ endothelial cells in glomerular capillaries were confirmed by the double-immunofluorescence method (Fig. 5g-i) and by transmission electron microscopy (Fig. 5j).

Morphological and immunohistochemical characteristics of LYVE-1$^+$ single cells in the interstitium

Figure 6 shows high magnification images of LYVE-1$^+$ single cells at various developmental ages. The cells had several thick irregular cytoplasmic processes that decreased gradually in diameter but increased in length after birth.

Figure 7 shows transmission electron micrographs of LYVE-1$^+$ single cells in the cortex (Fig. 7a-c) and medulla (Fig. 7d-f) at neonatal stage P4. These cells had a large irregular nucleus and many vesicles and vacuoles of various sizes in the cytoplasm. LYVE-1 was expressed on the plasma membrane and intracellular vesicles in these cells.

To test whether the single cells identified by LYVE-1 expression in the interstitium of the developing mouse kidney were macrophages, double-immunofluorescence studies were performed with the well-established macrophage markers F4/80 (mouse macrophage marker), CD11b (macrophage marker), and CD45 (common leukocyte marker; Fig. 8). Most of the LYVE-1$^+$ single cells in the interstitium of the developing mouse kidney were labeled with the mouse macrophage marker F4/80 (Fig. 8a), but not with CD45 (Fig. 8b), CD11b (Fig. 8c), nestin (Fig. 8d), or vimentin (Fig. 8e).

A histogram illustrating the number of LYVE-1$^+$ single cells in the interstitium, expressed per unit area, is shown in Fig. 9. The number of LYVE-1$^+$ cells increased markedly in the renal medulla immediately after birth and then gradually decreased from P7. LYVE-1$^+$ single cells had completely disappeared from the interstitium at P21.

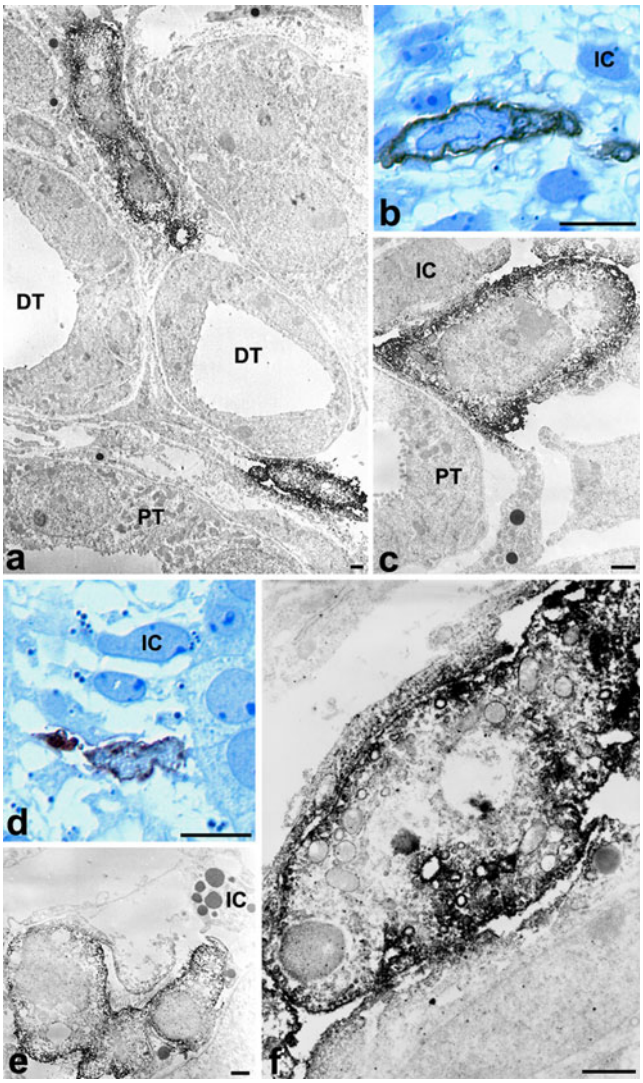

Fig. 7 Transmission electron micrographs (**a**, **c**, **e**, **f**) and light micrographs of a 1-μm plastic section stained with toluidine blue (**b**, **d**) illustrating LYVE-1$^+$ single cells in the cortex (**a–c**) and medulla (**d–f**) of the P4 kidney. LYVE-1 was expressed on the plasma membrane and the cytoplasmic vesicles. Note the large irregular nucleus of LYVE-1$^+$ single cells in both the cortex and medulla. No LYVE-1 immunoreactivity was detected in the proximal (*PT*) or distal (*DT*) tubule or in typical interstitial cells (*IC*) with an oval nucleus. *Bars* 10 μm (**b**, **d**), 1 μm (**a**, **c**, **e**, **f**)

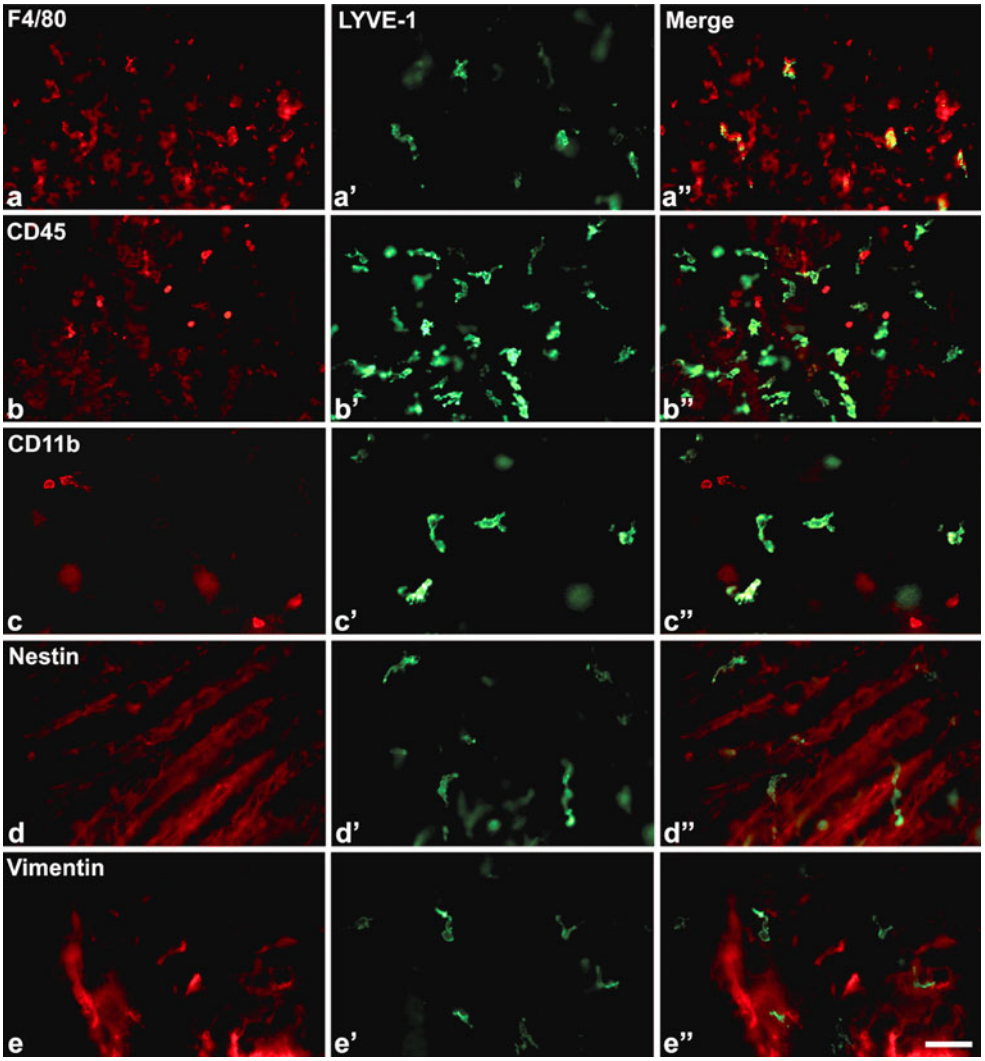

Fig. 8 Double-immunostaining for LYVE-1 and F4/80 (**a-a"**), LYVE-1 and CD45 (**b–b"**), LYVE-1 and CD11b (**c–c"**), LYVE-1 and nestin (**d–d"**), and LYVE-1 and vimentin (**e–e"**) in 4-day-old mouse kidneys. LYVE-1 was coexpressed in a subset of F4/80$^+$ macrophages (**a-a"**), but not in CD45$^+$ cells (**b–b"**), CD11b$^+$ cells (**c–c"**), nestin$^+$ cells (**d–d"**), or vimentin$^+$ cells (**e–e"**) in mouse kidneys. *Bars* 50 μm

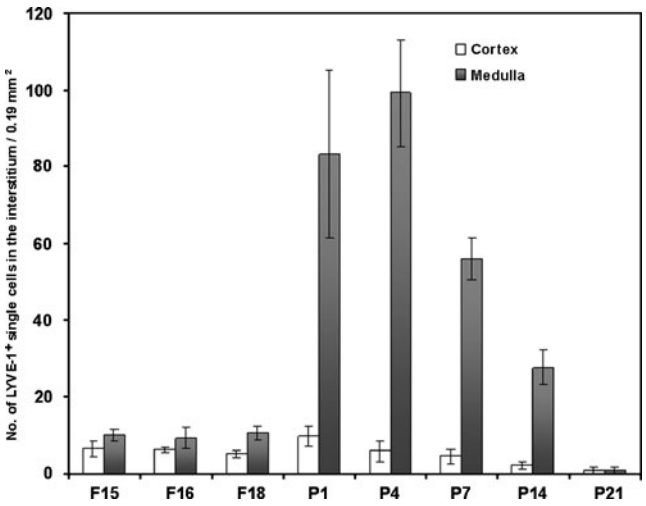

Fig. 9 Histogram of the number of LYVE-1$^+$ single cells in the interstitium per unit area. The numbers of LYVE-1$^+$ single cells increased markedly in the medulla immediately after birth but then reduced from P7 and disappeared completely by P21

Immunohistochemical detection of Prox1 in developing and adult mouse kidneys

We also used Prox1, a master regulator of lymphatic endothelial differentiation, to confirm whether the expression of Prox1 appeared in all LYVE-1$^+$ structures in the developing mouse kidney. Prox1 appeared in all LYVE-1$^+$ renal lymphatic vessels from E13 and continued to be expressed in adult mouse kidney, but not in a subset of LYVE-1$^+$ endothelial cells in glomerular capillaries and developing renal veins, or in F4/80$^+$/CD11b$^-$/LYVE-1$^+$ immature macrophages/dendritic cells (Fig. 10).

Discussion

This is the first description of the expression of the hyaluronan receptor LYVE-1 in the lymphatic vessels of the developing mouse kidney. In the adult mouse kidney, LYVE-1 is expressed mainly in the LECs and in a subset of

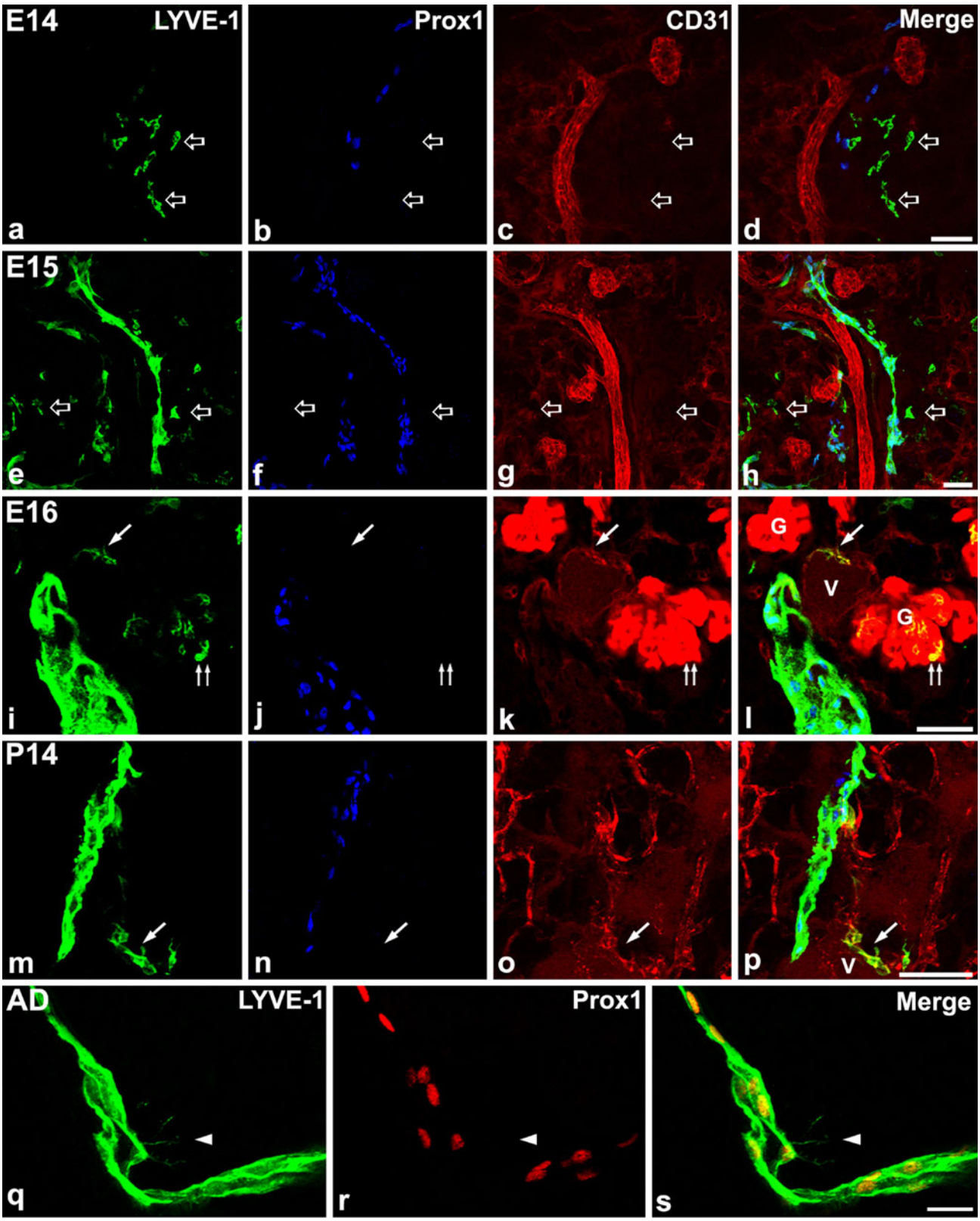

Fig. 10 Double- or triple-immunofluorescence staining of LYVE-1 (*green*), Prox1 (*blue* or *red*) or CD31 (*red*) in mouse kidneys from 14-day-old (**a–d**), 15-day-old (**e–h**), and 16-day-old (**i–l**) fetuses, 14-day-old (**m–p**) pups, and adults (**q–s**). **a–s** Prox1 is expressed only in the LYVE-1$^+$ lymphatic vessels from E14 to adulthood. No immunoreactivity for Prox1 is present in CD31$^+$ arterial or venous endothelial cells, in LYVE-1$^+$ single cells (*open arrows*), or in a subset of CD31$^+$/LYVE-1$^+$ endothelial cells (*double arrows* or *single arrows*) in glomerular capillaries (*G*) or arcuate veins (*V*). Note filopodia-like sprouts of growing lymphatic vessels (*arrowheads*). *Bars* 50 μm

endothelial cells of glomerular capillaries. However, in the developing mouse kidney, LYVE-1 is expressed not only in the LECs and glomerular capillaries, but also transiently in differentiating renal veins and in F4/80$^+$/CD11b$^-$ immature macrophages/dendritic cells in the interstitium. F4/80$^+$/CD11b$^-$/LYVE-1$^+$ immature macrophages/dendritic cells appear prior to the appearance of LYVE-1$^+$ lymphatic vessels and are closely intermingled or even form part of the lymphatic vascular wall. The extension of extra-renal LYVE-1$^+$ lymphatic vessels into the kidneys occurs at E13. The lymphatic plexus forms around the differentiating renal veins, which possess LYVE-1$^+$ branching buds during fetal and neonatal ages. Prox1 is expressed only in the LYVE-1$^+$ LECs from fetus to adulthood, but not in LYVE-1$^+$ endothelial cells of the renal vein and macrophages/dendritic cells.

Origin of lymphatic vessels in developing mouse kidney

In the developing mouse kidney, LYVE-1$^+$ lymphatic capillaries appear at E13 and form connections with extra-renal lymphatics. Prox1 expression in the LYVE-1$^+$ LECs is initiated at the same time (E13) and continues into adulthood. The constant expression of Prox1 in the embryonic and mature lymphatic vasculature is required throughout the life of LECs to maintain their differentiated identity (Bixel and Adams 2008; Johnson et al. 2008). These data suggest that lymphatic vessels in the kidney are derived from extensions of extra-renal lymphatic vessels through an active branching process.

To date, the hypothesis proposed by Florence Sabin about 100 years ago stating that LECs arise by sprouting from embryonic veins is the most widely accepted model of lymphangiogenesis (Sabin 1909; Srinivasan et al. 2007). In the mouse, LYVE-1 starts to be expressed in venous endothelial cells in the cardinal vein and currently provides the first indicator of lymphatic endothelial competence (Harvey and Oliver 2004; Jurisic and Detmar 2009; Maby-El Hajjami and Petrova 2008; Oliver 2004; Oliver and Detmar 2002; Wigle et al. 2002). Almost at the same time, Prox1 starts to be expressed in a restricted subpopulation of endothelial cells in the cardinal veins (an apparently obligatory step), and soon thereafter these LYVE-1$^+$/Prox1$^+$ cells begin to bud from the vein and migrate in a polarized manner, eventually forming lymph sacs (Oliver 2004; Wigle and Oliver 1999). In the developing renal veins, LYVE-1$^+$ endothelial cells appear from E14 to immediately after birth, especially in most of the branching buds. However, no Prox1 is expressed in these LYVE-1$^+$ venous endothelial cells. Interestingly, at these ages, most of the LYVE-1$^+$ lymphatic vessels with Prox1 immunoreactivity are located around the developing arcuate and interlobular veins. These results suggest that Prox1 might be not required to promote the initial budding from the veins, but instead might be necessary to maintain the endothelial budding and sprouting that will give rise to the lymphatic vessel, at least in developing mouse kidney.

Expression of LYVE-1 in F4/80$^+$/CD11b$^-$ macrophages

CD11b$^+$ or CD68$^+$ macrophages express the lymphatic endothelial marker LYVE-1, which might participate in lymphangiogenesis in the various pathological conditions that are involved in chronic inflammatory disease, transplant rejection, and tumorigenesis (Attout et al. 2009; Jeon et al. 2008; Maruyama et al. 2005; Rinda Soong et al. 2010; Schroedl et al. 2008). Schledzewski et al. (2006) and Maruyama et al. (2007) report that LYVE-1$^+$/CD11b$^+$ macrophages also express F4/80 in malignant tumors and in tissues undergoing wound healing. The present study has clearly demonstrated the expression of LYVE-1 in numerous interstitial cells with thick irregular cytoplasmic processes from E12 to P14. These cells are less numerous than F4/80$^+$ cells, but considerable overlap occurs because most of the LYVE-1$^+$ single cells also express F4/80. Surprisingly, neither CD45 nor CD11b is expressed on the LYVE-1$^+$ single cells in the developing mouse kidney. Numerous dendritic cell subpopulations have been defined by their expression of surface markers, such as myeloid dendritic cells that express CD11b or immature dendritic cell subsets that are positive for F4/80 (Austyn et al. 1994; Shortman and Liu 2002). Together, these data suggest that the LYVE-1$^+$ single cells in the developing mouse kidney are F4/80$^+$/CD11b$^-$ immature macrophages/dendritic cells. Interestingly, these F4/80$^+$/CD11b$^-$/LYVE-1$^+$ immature macrophages/dendritic cells are present before the appearance of LYVE-1$^+$ lymphatic vessels and are mainly localized to the outer part of the inner stripe of the outer medulla, whereas developing LYVE-1$^+$ lymphatic vessels are located in the cortex. Tissue macrophages are one of the sources for VEGF-C, which plays an important role in lymphangiogenesis in inflammatory and neoplastic conditions (Hirakawa et al. 2003; Kerjaschki 2007; Kriehuber et al. 2001; Petrova et al. 2002). This raises the possibility that F4/80$^+$/CD11b$^-$/LYVE-1$^+$ immature macrophages/dendritic cells contribute to lymphangiogenesis via the paracrine release of VEGF-C in the developing mouse kidney, a suggestion in agreement with previous findings showing that lymphangiogenesis is closely associated with a subtype of macrophages in the transplanted kidney and cornea (Cursiefen et al. 2004; Kerjaschki 2005a, b; Maruyama et al. 2005), in tumorigenesis (Schoppmann et al 2002), or in the rat remnant kidney model of cortical fibrosis (Matsui et al. 2003). Even though some F4/80$^+$/CD11b$^-$/LYVE-1$^+$ immature macrophages/dendritic cells have been observed around the developing lymphatic vessels, we have never seen the aggregation or formation of tube-like structures by these cells. However, it

is difficult to rule out that such cells might recruit circulation-derived lymphatic endothelial precursor cells and transdifferentiate into LECs (He et al. 2004), because some of these cells are directly connected with developing renal lymphatic vessels. In view of the electron-microscopic findings that LYVE-1 is expressed not only on the plasma membrane, but also on the intracellular vesicles and vacuoles in these cells, we speculate that these cells are involved in the degradation of hyaluronan in the medulla during development. In mature kidney, interstitial fluid is cleared from the medullary interstitium through the ascending vasa recta (Madsen et al. 2008).

Expression of LYVE-1 on a subset of glomerular endothelial cells

Another interesting finding in this study is that LYVE-1 is expressed on a subset of endothelial cells of the glomerular capillary in the adult mouse kidney. LYVE-1$^+$ endothelial cells appear first in the glomeruli of stage III nephrons at E15 in the developing mouse kidney. LYVE-1 is known to be able to mediate the uptake of hyaluronan in vitro, as shown by the internalization of fluorescein-isothiocyanate–labeled hyaluronan by LYVE-1-transfected fibroblasts (Prevo et al. 2001). Taken together with the finding that LYVE-1 is present on both the luminal and abluminal plasma membranes of these endothelial cells, we speculate that LYVE-1$^+$ endothelial cells in the glomerular capillary play a role in transporting hyaluronan from the mesangial matrix to the capillary lumen by transcytosis. The observation that soluble CD44 molecules can bind effectively to hyaluronan sequestered by immobilized LYVE-1 in vitro (Banerji et al. 1999) suggests that LYVE-1$^+$ endothelial cells also provide a pathway for extra/intravasation of CD44$^+$ leukocytes in the glomeruli.

The role of LYVE-1 in the regulation of lymphatic vascular function is not known, but mice lacking this receptor have normal lymphatic vessels and lack any defect in constitutive dendritic cell trafficking (Gale et al. 2007). These results suggest that LYVE-1 is not obligatory for normal lymphatic development and may play a role more specific than that of the established function of LYVE-1, namely the uptake or transport of hyaluronan across the lymphatic wall (Jackson et al. 2001; Prevo et al. 2001).

Concluding remarks

We propose that lymphatic vessels in the developing mouse kidney arise mainly from pre-existing extra-renal lymphatic vessels through an active branching process. Moreover, LYVE-1$^+$ venous endothelial cells and F4/80$^+$/CD11b$^-$/LYVE-1$^+$ immature macrophages/dendritic cells might also play a role in renal lymphangiogenesis.

Acknowledgments The authors are grateful to Dr. Craig C. Tisher and Kirsten M. Madsen (University of Florida) for advice during this study and also thank Hong-Lim Kim for technical assistance.

References

Al-Rawi MA, Mansel RE, Jiang WG (2005) Molecular and cellular mechanisms of lymphangiogenesis. Eur J Surg Oncol 31:117–121

Alitalo K, Tammela T, Petrova TV (2005) Lymphangiogenesis in development and human disease. Nature 38:946–953

Attout T, Hoerauf A, Dénécé G, Debrah AY, Marfo-Debrekyei Y, Boussinesq M, Wanji S, Martinez V, Mand S, Adjei O, Bain O, Specht S, Martin C (2009) Lymphatic vascularisation and involvement of Lyve-1+ macrophages in the human onchocerca nodule. PLoS ONE 4:e8234

Austyn JM, Hankins DF, Larsen CP, Morris PJ, Rao AS, Roake JA (1994) Isolation and characterization of dendritic cells from mouse heart and kidney. J Immunol 152:2401–2410

Banerji S, Ni J, Wang SX, Clasper S, Su J, Tammi R, Jones M, Jackson DG (1999) LYVE-1, a new homologue of the CD44 glycoprotein, is a lymph-specific receptor for hyaluronan. J Cell Biol 144:789–801

Beasley NJ, Prevo R, Banerji S, Leek RD, Moore J, Van Tranppen P, Cox G, Harris AL, Jackson DG (2002) Intratumoral lymphangiogenesis and lymph node metastasis in head and neck cancer. Cancer Res 62:1315–1320

Bixel MG, Adams RH (2008) Master and commander: continued expression of Prox1 prevents the dedifferentiation of lymphatic endothelial cells. Genes Dev 22:3282–3291

Bouwens L, DeBlay E (1996) Islet morphogenesis and stem cell markers in rat pancreas. J Histochem Cytochem 44:947–951

Cursiefen C, Chen L, Borges LP, Jackson D, Cao J, Radziejewski C, D'Amore PA, Dana MR, Wiegand SJ, Streilein JW (2004) VEGF-A stimulates lymphangiogenesis and hemangiogenesis in inflammatory neovascularization via macrophage recruitment. J Clin Invest 113:1040–1050

Cuttino JT Jr, Jennette JC, Clark RL, Kwock L (1985) Renal medullary lymphatics: microrediographic, light, and electron microscopic studies in pigs. Lymphology 18:24–30

Gale NW, Prevo R, Espinosa J, Ferguson DJ, Dominguez MG, Yancopoulod GD, Thurston G, Jackson DG (2007) Normal lymphatic development and function in mice deficient for the lymphatic hyaluronan receptor LYVE-1. Mol Cell Biol 27:595–604

Grant AJ, Goddard S, Ahmed-Choudhury J, Reynolds G, Jackson DG, Briskin M, Wu L, Hübscher SG, Adams DH (2002) Hepatic expression of secondary lymphoid chemokine (CCL21) promotes the development of portal-associated lymphoid tissue in chronic inflammatory liver disease. Am J Pathol 160:1445–1455

Hamrah P, Chen L, Cursiefen C, Zhang Q, Joyce NC, Dana MR (2004) Expression of vascular endothelial growth factor receptor-3 (VEGFR-3) on monocytic bone marrow-derived cells in the conjunctiva. Exp Eye Res 79:553–561

Harvey NL, Oliver G (2004) Choose your fate: artery, vein or lymphatic vessel? Curr Opin Genet Dev 14:499–505

He Y, Rajantie I, Ilmonen M, Makinen T, Karkkainen MJ, Haiko P, Salven P, Alitalo K (2004) Preexisting lymphatic endothelium but not endothelial progenitor cells are essential for tumor lymphangiogenesis and lymphatic metastasis. Cancer Res 64:3737–3740

Hirakawa S, Detmar M (2004) New insights into the biology and pathology of the cutaneous lymphatic system. J Dermatol Sci 35:1–8

Hirakawa S, Hong YK, Harvey N, Schacht V, Matsuda K, Libermann T, Detmar M (2003) Identification of vascular lineage-specific genes by transcriptional profiling of isolated blood vascular and lymphatic endothelial cells. Am J Pathol 162:575–586

Hogg CM, Reid O, Scothorne RJ (1982) Studies on hemolymph nodes. III. Renal lymph as a major source of erythrocytes in the renal hemolymph node of the rat. J Anat 135:291–299

Holmes MJ, O'Morchoe PJ, O'Morchoe CC (1977) Morphology of the intrarenal lymphatic system. Capsular and hilar communications. Am J Anat 149:333–351

Jackson DG (2004) Biology of the lymphatic marker LYVE-1 and applications in research into lymphatic trafficking and lymphangiogenesis. APMIS 112:526–538

Jackson DG, Prevo R, Clasper S, Banerji S (2001) LYVE-1, the lymphatic system and tumor lymphangiogenesis. Trends Immunol 22:317–321

Jeon BH, Jang C, Han J, Kataru RP, Piao L, Jung K, Cha HJ, Schwendener RA, Jang KY, Kim KS, Alitalo K, Koh GY (2008) Profound but dysfunctional lymphangiogenesis via vascular endothelial growth factor ligands from CD11b+macrophages in advanced ovarian cancer. Cancer Res 68:1100–1109

Johnson NC, Dillard ME, Baluk P, McDonald DM, Harvey NL, Frase SL, Oliver G (2008) Lymphatic endothelial cell identity is reversible and its maintenance requires Prox1 activity. Genes Dev 22:3232–3235

Jurisic G, Detmar M (2009) Lymphatic endothelium in health and disease. Cell Tissue Res 335:97–108

Kerjaschki D (2005a) Lymphatic neoangiogenesis in human neoplasia and transplantation as experiments of nature. Kidney Int 68:1967–1968

Kerjaschki D (2005b) The crucial role of macrophages in lymphangiogenesis. J Clin Invest 115:2316–2319

Kerjaschki D (2007) How to control lymphangiogenesis: a novel role for rapamycin. Kidney Int 71:717–719

Kim J, Kim WY, Han KH, Knepper MA, Nielsen S, Madsen KM (1999) Developmental expression of aquaporin 1 in the rat renal vasculature. Am J Physiol Renal Physiol 276:F498–F509

Kriehuber E, Breiteneder-Geleff S, Groeger M, Soleiman A, Schoppmann SF, Stingl G, Kerjaschki D, Maurer D (2001) Isolation and characterization of dermal lymphatic and blood endothelial cells reveal stable and functionally specialized cell lineages. J Exp Med 194:797–808

Kubo H, Fujiwara T, Jussila L, Hashi H, Ogawa M, Shimizu K, Awane M, Sakai Y, Takabayashi A, Alitalo K, Yamaoka Y, Nishikawa SI (2000) Involvement of vascular endothelial growth factor receptor-3 in maintenance of integrity of endothelial cell lining during tumor angiogenesis. Blood 96:546–553

Lendahl U, Zimmerman LB, McKay RD (1990) CNS stem cells express a new class of intermediate filament protein. Cell 60:585–595

Maby-El Hajjami H, Petrova TV (2008) Developmental and pathological lymphangiogenesis: from models to human disease. Histochem Cell Biol 130:1063–1078

Madsen KM, Nielsen S, Tisher CC (2008) Anatomy of the kidney. In: Brenner BM (ed) Brenner and Rector's The kidney, vol 1, Lymphatics. Saunders Elsevier, Philadelphia, pp 25–90

Maruyama K, Li M, Cursiefen C, Jackson DG, Keino H, Tomita M, Rooijen NV, Takenaka H, D'Amore PA, Stein-Streilein J, Losordo DW, Streilein JW (2005) Inflammation-induced lymphangiogenesis in the cornea arises from CD11b-positive macrophages. J Clin Invest 115:2363–2372

Maruyama K, Asai J, Ii M, Thorne T, Losordo DW, D'Amore PA (2007) Decreased macrophage number and activation lead to reduced lymphatic vessel formation and contribute to impaired diabetic wound healing. Am J Pathol 170:1178–1191

Matsui K, Nagy-Bojarsky K, Laakkonen P, Krieger S, Mechtler K, Uchida S, Geleff S, Kang DH, Johnson RJ, Kerjaschki D (2003) Lymphatic microvessels in the rat remnant kidney model of renal fibrosis: aminopeptidase P and podoplanin are discriminatory markers for endothelial cells of blood and lymphatic vessels. J Am Soc Nephrol 14:1981–1989

Mouta Carreira C, Nasser SM, Tomaso E di, Padera TP, Boucher Y, Tomarev SI, Jain RK (2001) LYVE-1 is not restricted to the lymph vessels expression in normal liver blood sinusoids and down-regulation in human liver cancer and cirrhosis. Cancer Res 61:8079–8084

Niki T, Iba S, Yamada T, Matsuno Y, Enholm B, Hirohashi S (2001) Expression of vascular endothelial growth factor receptor 3 in blood and lymphatic vessels of lung adenocarcinoma. J Pathol 193:450–457

Oliver G (2004) Lymphatic vasculature development. Nat Rev Immunol 4:35–45

Oliver G, Detmar M (2002) The rediscovery of lymphatic system: old and new insights into the development and biological function of the lymphatic vasculature. Genes Dev 16:773–784

Oliver G, Alitalo K (2005) The lymphatic vasculature: recent progress and paradigms. Annu Rev Cell Dev Biol 21:457–483

Petrova TV, Makinen T, Makela TP, Saarela J, Virtanen I, Ferrell RE, Finegold DN, Kerjaschki D, Yla-Herttuala S, Alitalo K (2002) Lymphatic endothelial reprogramming of vascular endothelial cells by the Prox-1 homeobox transcriptin factor. EMBO J 21:4593–4599

Prevo R, Banerji S, Ferguson D, Jackson DG (2001) Mouse LYVE-1 is an endocytic receptor for hyaluronan in lymphatic endothelium. J Biol Chem 276:19420–19430

Pure E, Cuff CA (2001) A crucial role for CD44 in inflammation. Trends Mol Med 7:213–221

Rinda Soong T, Pathak AP, Asano H, Fox-Talbot K, Baldwin WM 3rd (2010) Lymphatic injury and regeneration in cardiac allografts. Transplantation 89:500–508

Rohn DA, Stewart RH, Elk JR, Laine GA, Drake RE (1996) Renal lymphatic function following venous pressure elevation. Lymphology 29:67–75

Sabin FR (1909) The lymphatic system in human embryos, with a consideration of the morphology of the system as a whole. Am J Anat 9:43–91

Schacht V, Dandras SS, Johnson LA, Jackson DG, Hong YK, Detmar M (2005) Up-regulation of the lymphtic marker podoplanin, a mucin-type transmembrane glycoprotein, in human squamous cell carcinomas and germ cell tumors. Am J Pathol 166:913–921

Schledzewski K, Falkowski M, Moldenhauer G, Metharom P, Kzhyshkowska J, Ganss R, Demory A, Falkowska-Hansen B, Kurzen H, Ugurel S, Geginat G, Arnold B, Goerdt S (2006) Lymphatic endothelium-specific hyaluronan receptor LYVE-1 is expressed by stabilin-1^+, F4/80^+, CD$11b^+$ macrophages in malignant tumours and wound healing tissue in vivo and in bone marrow cultures in vitro: implications for the assessment of lymphangiogenesis. J Pathol 209:67–77

Schoppmann SF, Birner P, Stöckl J, Kalt R, Ullrich R, Caucig C, Kriehuber E, Nagy K, Alitalo K, Kerjaschki D (2002) Tumor-associated macrophages express lymphatic endothelial growth factors and are related to peritumoral lymphangiogenesis. Am J Pathol 161:947–956

Schroedl F, Brehmer A, Neuhuber WL, Kruse FE, May CA, Cursiefen C (2008) The normal human choroid is endowed with a significant number of lymphatic vessel endothelial hyaluronate receptor 1 (LYVE-1)-positive macrophages. Invest Ophthalmol Vis Sci 49:5222–5229

Shortman K, Liu YJ (2002) Mouse and human dendritic cell subtypes. Nat Rev Immunol 2:151–161

Srinivasan RS, Dillard ME, Lagutin OV, Lin FJ, Tsai S, Tsai MJ, Samokhvalov IM, Oliver G (2007) Lineage tracing demonstrates the venous origin of the mammalian lymphatic vasculature. Genes Dev 21:2422-2432 (Comment in Lymphat Res Biol 5:275–276)

Tammela T, Petrova TV, Alitalo K (2005) Molecular lymphangiogenesis: new players. Trends Cell Biol 15:434–441

Wigle JT, Oliver G (1999) Prox1 function is required for the development of the murine lymphatic system. Cell 98:769–778

Wigle JT, Harvey N, Detmar M, Lagurina I, Grosveld G, Gunn MD, Jackson DG, Oliver G (2002) An essential role for Prox1 in the induction of the lymphatic endothelial cell phenotype. EMBO J 21:1505–1513